



DPNC, University of Geneva – PhD Defense

# Development of the next generation space-based Compton polarimeter and energy resolved polarization analysis of GRBs' prompt emission

Nicolas De Angelis

Supervisors: Prof. Xin Wu, Dr. Merlin Kole

December 7, 2023

[Link to Manuscript](#)





# Outline

- ① Gamma-Ray Bursts and Polarization
- ② Energy-Resolved GRB Polarization Analysis with POLAR
- ③ Design and Development of the POLAR-2 Instrument
- ④ Temperature Dependent Radiation Damage Annealing of Silicon PhotoMultipliers
- ⑤ Optical Characterization, Simulation, and Calibration of the POLAR-2 Polarimeter Modules



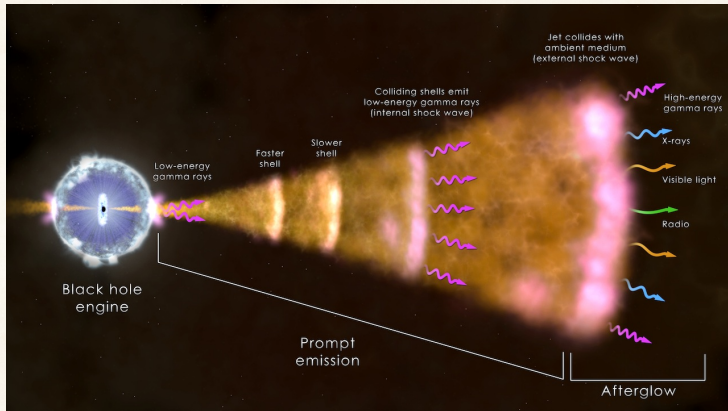
A detailed 3D rendering of a satellite in orbit around Earth. The satellite features a large white cylindrical body with various scientific instruments attached. A prominent feature is a white parabolic dish antenna mounted on a white cylindrical base. To the right, there are two large rectangular solar panels with a grid of blue cells. The background shows the blue and white atmosphere of Earth's horizon. In the foreground, a central instrument is shown with a grid of small green lights or sensors.

## Section 1

# Gamma-Ray Bursts and Polarization

# The Gamma-Ray Bursts paradigm

- Bright and short transient event in the  $\gamma$  band (**prompt emission**) followed by an **afterglow** spanning the entire EM spectrum

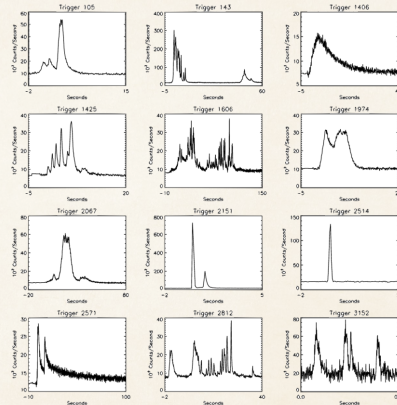


(Credit: NASA's Goddard Space Flight Center)



# The Gamma-Ray Bursts paradigm

- Bright and short transient event in the  $\gamma$  band (**prompt emission**) followed by an **afterglow** spanning the entire EM spectrum

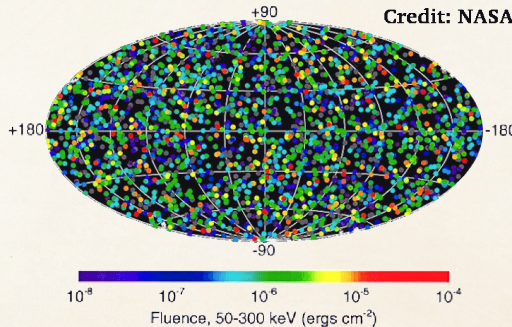


(Credit: J.T. Bonnell (NASA/GSFC))



# The Gamma-Ray Bursts paradigm

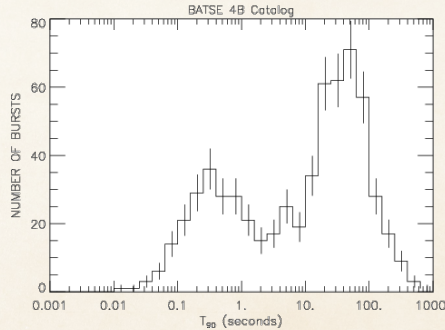
- Bright and short transient event in the  $\gamma$  band (**prompt emission**) followed by an **afterglow** spanning the entire EM spectrum
- GRBs are uniformly distributed in the sky, have very diverse spectral properties and fluence, and are of extragalactic origin





# The Gamma-Ray Bursts paradigm

- Bright and short transient event in the  $\gamma$  band (**prompt emission**) followed by an **afterglow** spanning the entire EM spectrum
- GRBs are uniformly distributed in the sky, have very diverse spectral properties and fluence, and are of extragalactic origin
- Classified in two categories: short GRBs ( $T_{90} < 2$  s) are originated by binary compact object merger, long ones ( $T_{90} > 2$  s) are associated with supermassive star explosions

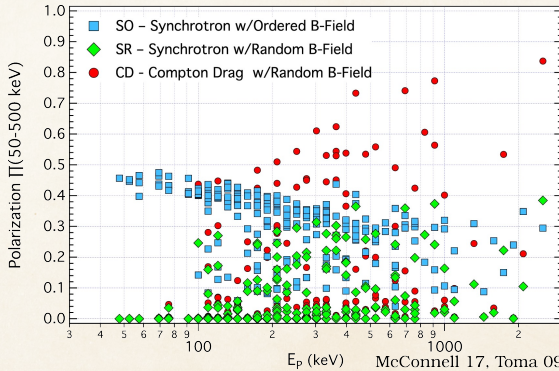


(Credit: BATSE 4B Catalog, Robert S. Mallozzi)

# Why measuring GRB polarization ?

Spectral information alone does not allow to disentangle the existing emission models.  
Measuring polarization is a very powerful tool to probe the physics of GRBs, as it can inform us about:

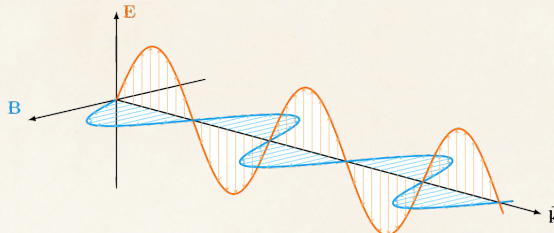
- ⌚ The emission mechanism at play in the source (synchrotron vs. photospheric)
- ⌚ The outflow dynamics: Kinetic Energy vs. Poynting Flux Dominated
- ⌚ The jet angular structure: top hat jet, with smooth edges, truly structured
- ⌚ The magnetic field configuration (random, ordered)





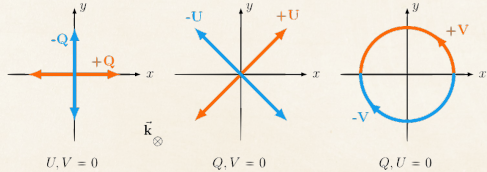
# Polarization of Electro-Magnetic Waves

## Stokes Parameterization



A photon consists of the propagation of orthogonal **E** and **B** fields. **E** is taken by convention as the polarization vector. Stokes parameterization of the polarization state:

$$\vec{S} = \begin{cases} S_0 \equiv I = \langle E_x^2 \rangle + \langle E_y^2 \rangle \\ S_1 \equiv Q = \langle E_x^2 \rangle - \langle E_y^2 \rangle \\ S_2 \equiv U = \langle E_{45^\circ}^2 \rangle - \langle E_{-45^\circ}^2 \rangle \\ S_3 \equiv V = \langle E_R^2 \rangle - \langle E_L^2 \rangle \end{cases}$$



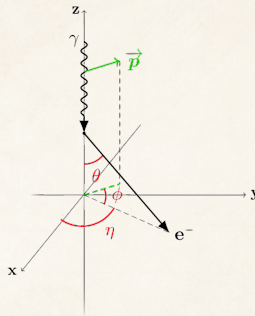
For a linearly polarized wave, polarization degree and angle are defined by:

$$p = \frac{\sqrt{Q^2 + U^2}}{I}; \quad \psi = \frac{1}{2} \arctan \frac{U}{Q}$$

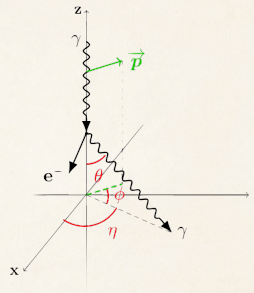
# Photon interaction with matter

- Photon interacts with matter through three processes:

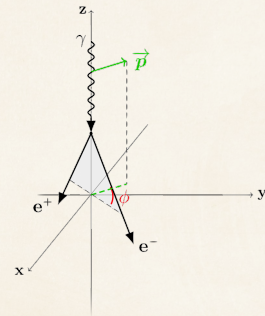
Photo-electric effect



Compton scattering



Pair production



- Each process is dominant at different energies
- The azimuthal distribution of the secondary products is correlated with the polarization direction of the primary photon:  $\frac{d\sigma}{d\Omega} \propto 1 + \mu \cos(2\phi)$

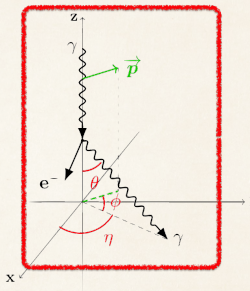
# Photon interaction with matter

- Photon interacts with matter through three processes:

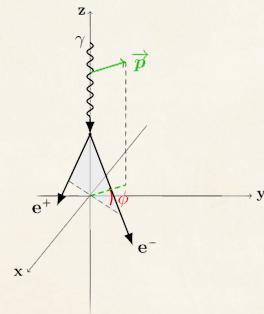
Photo-electric effect



Compton scattering



Pair production



- Each process is dominant at different energies
- The azimuthal distribution of the secondary products is correlated with the polarization direction of the primary photon:  $\frac{d\sigma}{d\Omega} \propto 1 + \mu \cos(2\phi)$
- We focus here on the Compton scattering process, dominant in the energy band where the prompt emission peaks



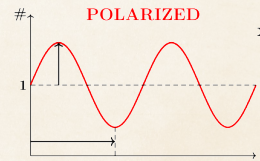
# Compton Polarimetry

Compton scattering can be used to determine the polarization of a source:

- ⌚ Azimuthal scattering angle distribution provides information on PD and PA
- ⌚ Modulation curve parameterized by the Klein-Nishina cross-section:

$$\frac{d\sigma}{d\Omega} = \frac{r_e^2}{2} \left( \frac{E'}{E} \right)^2 \left[ \frac{E'}{E} + \frac{E}{E'} - 2 \sin^2(\theta) \cos^2(\phi) \right]$$

- ⌚ Relative amplitude  $\leftrightarrow$  PD, phase  $\leftrightarrow$  PA



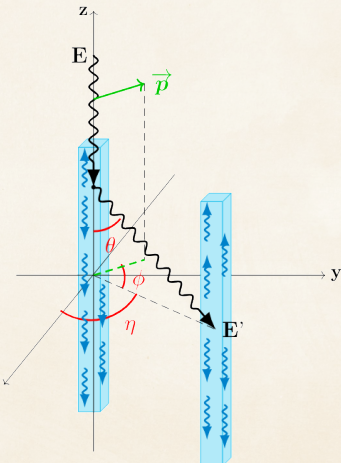
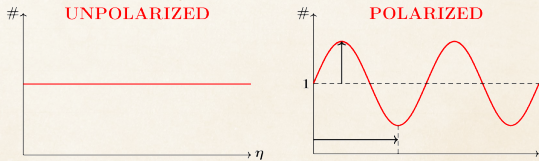
# Compton Polarimetry

Compton scattering can be used to determine the polarization of a source:

- ⌚ Azimuthal scattering angle distribution provides information on PD and PA
- ⌚ Modulation curve parameterized by the Klein-Nishina cross-section:

$$\frac{d\sigma}{d\Omega} = \frac{r_e^2}{2} \left( \frac{E'}{E} \right)^2 \left[ \frac{E'}{E} + \frac{E}{E'} - 2 \sin^2(\theta) \cos^2(\phi) \right]$$

- ⌚ Relative amplitude  $\leftrightarrow$  PD, phase  $\leftrightarrow$  PA
- ⌚ A segmented array of scintillators can be used to measure the scattering angle distribution (aka modulation curve)



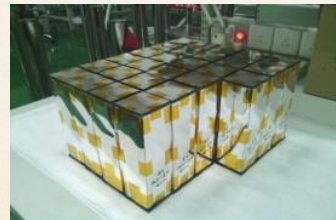
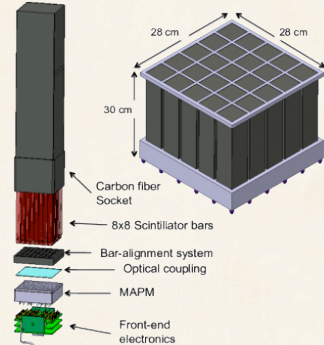


## Section 2

# Energy-Resolved GRB Polarization Analysis with POLAR

# The POLAR Instrument

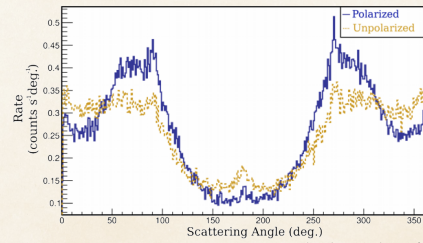
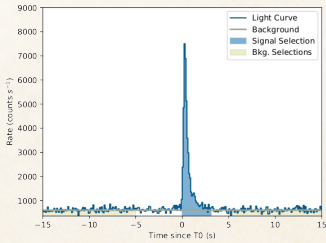
- ★ POLAR was a dedicated gamma polarimeter composed of a  $40 \times 40$  scintillator array
- ★ Divided in  $5 \times 5$  modules each made of 64 plastic scintillator bars ( $176 \times 5.8 \times 5.8 \text{ mm}^3$ , EJ-248M), each module being readout by Multi-Anode PMTs
- ★ Optimized for Compton scattering in the 50-500keV range thanks to its low-Z scintillators
- ★ 30kg instrument, half-sky FoV,  $\sim 300\text{cm}^2$  effective area at 400 keV
- ★ Design described in Produit et al. 2018 (DOI: [10.1016/j.nima.2017.09.053](https://doi.org/10.1016/j.nima.2017.09.053))
- ★ Launched in Sept 2016 on the Tiangong-2 Chinese space lab for 6 months of operation





# POLAR Results Prior to this Thesis

- Typical measured light and modulation curves shown below, complex modulation curve structure due to well-understood instrumental/geometrical effects
- POLAR detected 55 GRBs in 6 months of operation, 14 of which had enough statistics to be analyzed → joint spectral/polarization analysis with Fermi-GBM or Swift-BAT data using 3ML spectral fitting framework ([github.com/threeML](https://github.com/threeML)) and development of a polarization fitting plugin ([github.com/grburgess/polarpy](https://github.com/grburgess/polarpy))

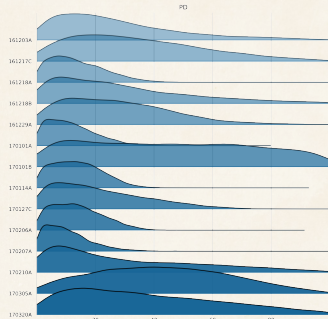


A&A 644, A124 (2020)

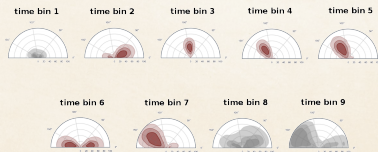


# POLAR Results Prior to this Thesis

- ★ Catalog of 14 GRBs analysed, results show a low or null polarization degree (excluding synchrotron emission models from toroidal magnetic field, compatible with photospheric emission model and other synchrotron models)
- ★ Time resolved analysis show a hint of quickly evolving polarization angle that washes out polarization degree on time integrated analysis
- ★ More statistics is needed in order to perform precise temporal and energy resolved analysis, with lowered energy threshold to probe emission models, and with bigger effective area and longer mission operation to get a larger catalog → **the POLAR-2 mission**



A&A 644, A124 (2020)

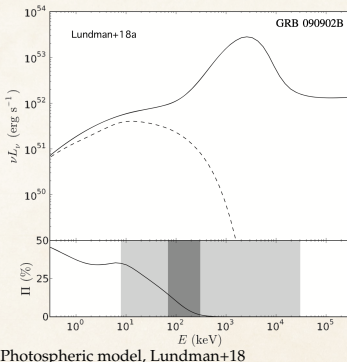


A&A 627, A105 (2019)

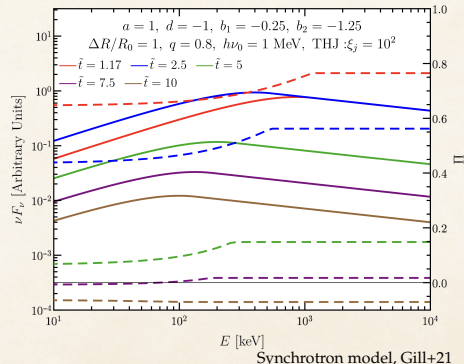
# Theoretical Predictions

## Energy Dependence of Polarization

- Energy-resolved polarimetric measurement made possible by increasing sensitivity of high energy polarimeters
- Theoretical models recently started to be extended to predict energy dependence of GRB prompt emission polarization



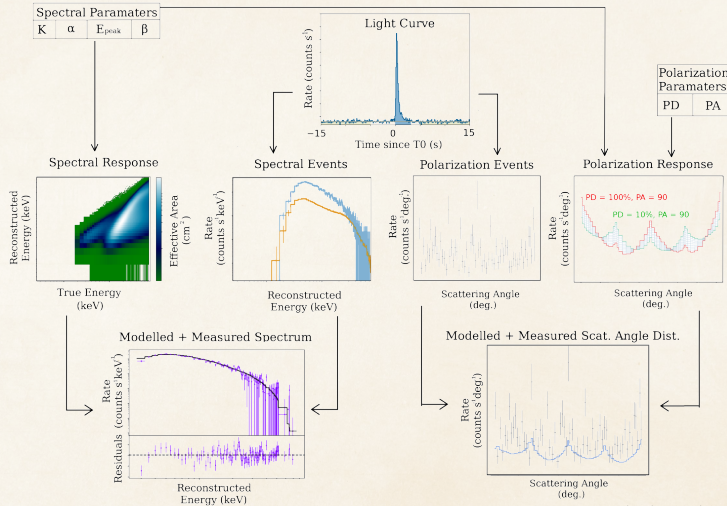
Photospheric model, Lundman+18



Synchrotron model, Gill+21

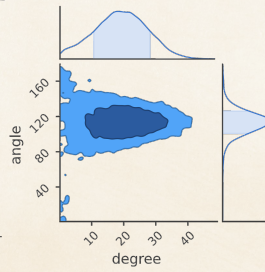
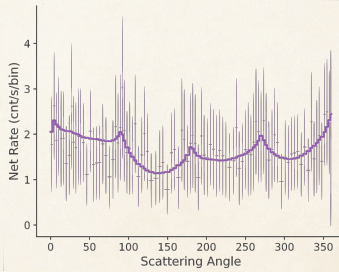
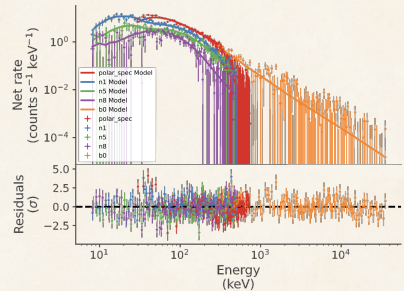
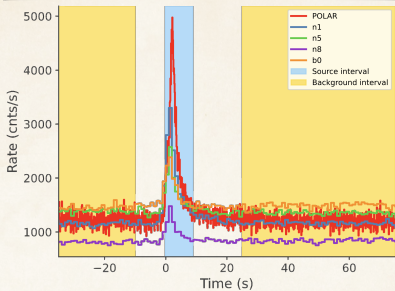
# GRB Analysis Workflow

Spectral and polarization events are fitted in parallel using a forward folding method. The spectral part is jointly fitted with Fermi-GBM/Swift-BAT data.





# Energy integrated results: GRB170114A

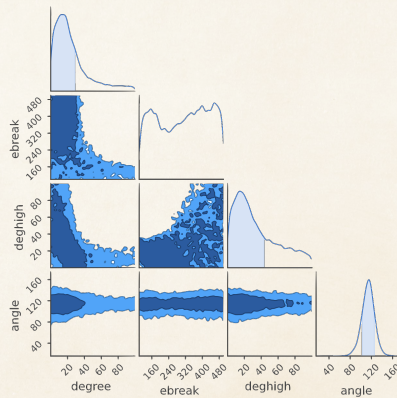


# Energy resolved results: GRB170114A

## Heaviside fit of the PD

Fitting the PD using two energy bins (using complex functions is not possible due to limited statistics):

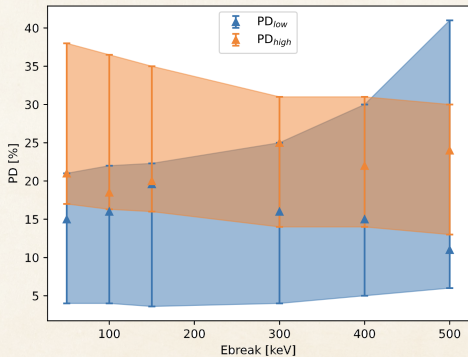
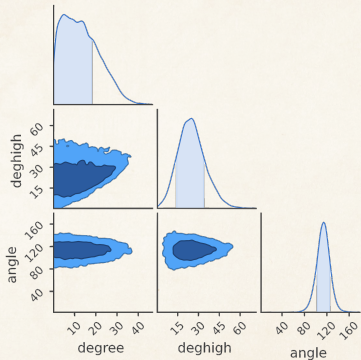
$$PD = \begin{cases} PD_{low} & \text{if } E < E_{break} \\ PD_{high} & \text{if } E > E_{break} \end{cases}; \quad PA = cst.$$



# Energy resolved results: GRB170114A

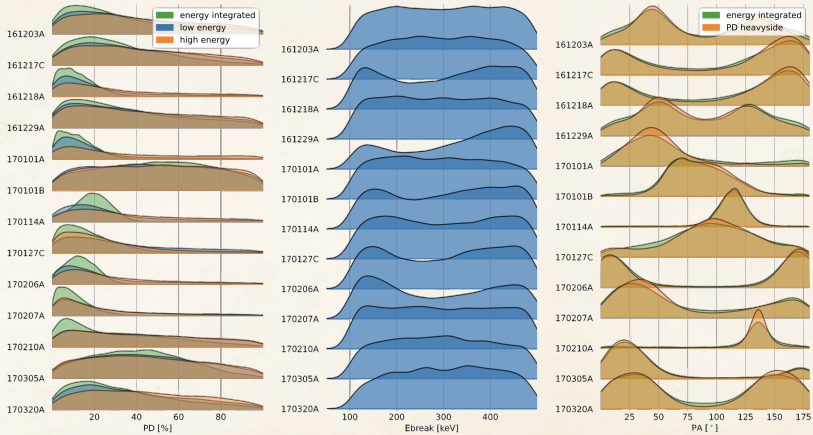
## Heaviside fit of the PD, fixed break

$$PD = \begin{cases} PD_{low} & \text{if } E < 150 \text{ keV} \\ PD_{high} & \text{if } E > 150 \text{ keV} \end{cases}; \quad PA = cst.$$



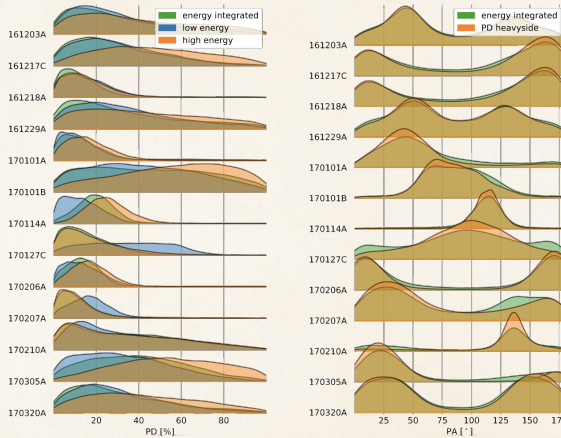


# Energy resolved results: POLAR catalog Heaviside fit of the PD



# Energy resolved results: POLAR catalog

## Heaviside fit of the PD, $E_{break} = 150$ keV



PD and PA were also fitted versus energy using a linear function, no significant energy dependence was found.



# What next ?

- ❖ No significant energy dependence of the polarization parameters was observed with the POLAR data
- ❖ Implement the energy-dependent fitting in a more generic way, such that not only empirical functions can be used but also actual energy-dependent theoretical models
- ❖ Compare the sensitivity of POLAR vs. POLAR-2 to energy dependence of polarization using fake GRBs
- ❖ Higher quality measurements are needed for time and energy resolved polarization analysis: **POLAR-2**



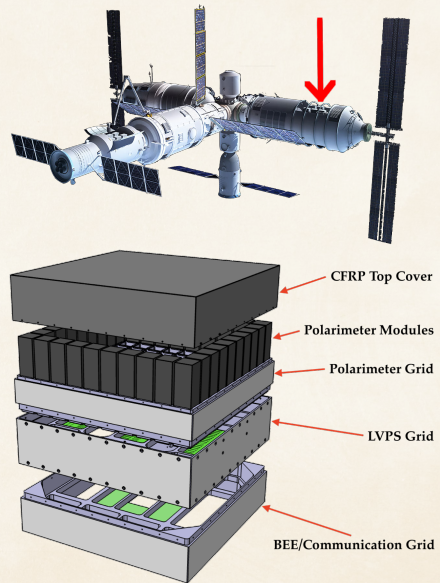
## Section 3

# Design and Development of the POLAR-2 Instrument



# The POLAR-2 instrument

- ◆ Large scale GRB polarimeter based on POLAR's legacy
- ◆ 4 times bigger than POLAR (from 25 to 100 polarimeter modules), 10 times more sensitive (thanks to an improved design)
- ◆ Lowered energy threshold down to a few keV
- ◆ Two other payloads (low energy polarimeter and spectral imager) being developed
- ◆ Planned for a launch to the CSS





# The POLAR-2 collaboration

About 20 people working on POLAR-2 from 4 countries:

- ◆ **UniGe (DPNC), Switzerland:** Management, polarimeter modules, instrument thermal and mechanical integration
- ◆ **UniGe (DA), Switzerland:** Online software system
- ◆ **NCBJ, Poland:** Back-End Electronics, Power Supply
- ◆ **IHEP, China:** Flight Model Acceptance, Spectrometers
- ◆ **MPE, Germany:** Qualification & Verification, Spectrometers



More information: <https://www.unige.ch/dpnc/polar-2>.



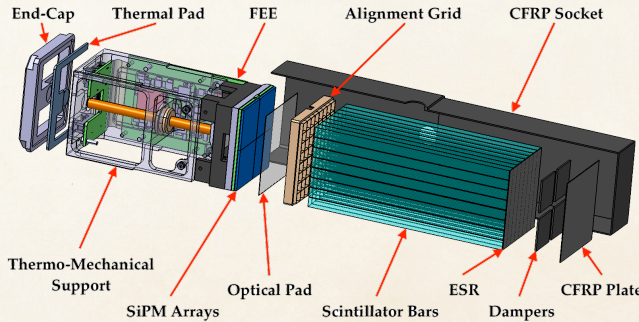
Max-Planck-Institut für  
extraterrestrische Physik



# Polarimeter Module Design

A polarimeter module consists of an  $8 \times 8$  array of individually wrapped plastic scintillator bars read out by SiPM arrays. The optical efficiency of the module has been greatly improved thanks to several upgrades:

- ◆ SiPMs instead of MA-PMTs: peak PDE increased from 0.2 to 0.5
- ◆ Scintillators reshaped: shorter (better SNR), wider (less dead volume), non-truncated (thanks to very thin mechanical grid, better light yield)
- ◆ Improved wrapping, thinner optical coupling pad: crosstalk reduced by an order of magnitude

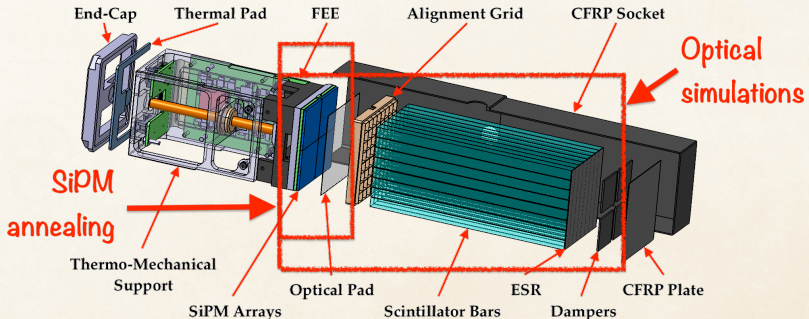




# Polarimeter Module Design

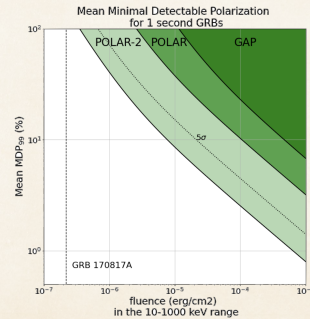
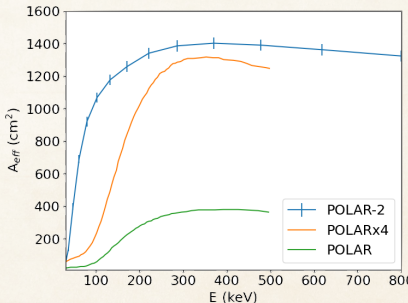
A polarimeter module consists of an  $8 \times 8$  array of individually wrapped plastic scintillator bars read out by SiPM arrays. The optical efficiency of the module has been greatly improved thanks to several upgrades:

- ◆ SiPMs instead of MA-PMTs: peak PDE increased from 0.2 to 0.5
- ◆ Scintillators reshaped: shorter (better SNR), wider (less dead volume), non-truncated (thanks to very thin mechanical grid, better light yield)
- ◆ Improved wrapping, thinner optical coupling pad: crosstalk reduced by an order of magnitude



# Anticipated Science Performances

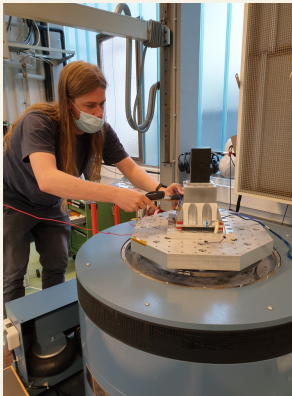
- ◆ Effective area greatly increased, especially at low energies, thanks to the improved module light yield
- ◆ Improvement of the modulation factor  $\mu_{100}$  (sensitivity to polarization) compared to POLAR
- ◆ About 50 GRBs/year with quality equal or higher than the best POLAR measurements
- ◆ POLAR-2 is sensitive to lower levels of polarization for weaker GRBs

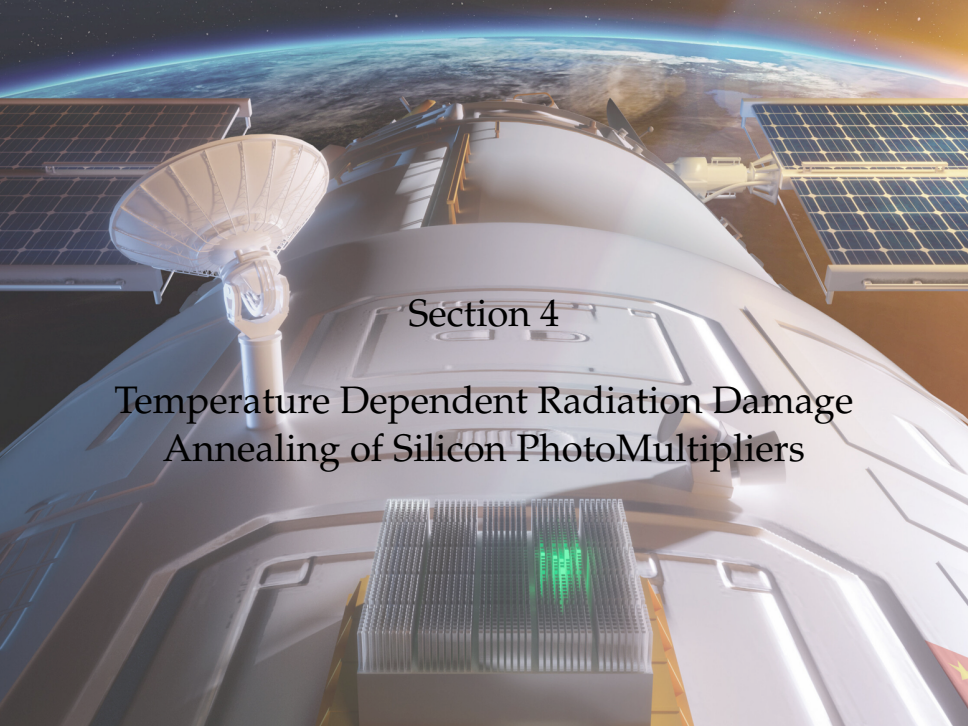


Galaxies 2021, 9, 82.

# POLAR-2 Space Qualification

Many component- and module-level space qualification tests: thermal vacuum cycling, vibration and shock tests, irradiation campaigns etc.



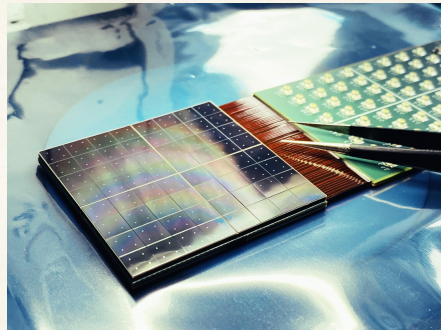
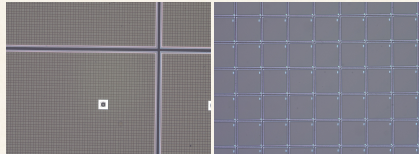


## Section 4

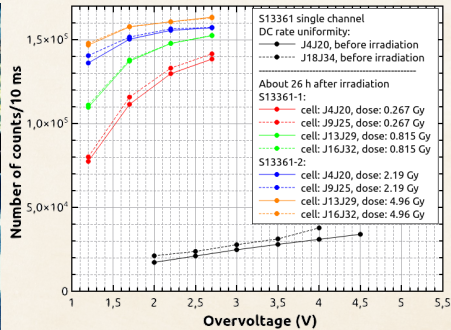
# Temperature Dependent Radiation Damage Annealing of Silicon PhotoMultipliers

# Silicon Photo-Multipliers Radiation Damage

Radiation damages SiPMs by inducing defects in the silicon lattice, leading to a higher DCR and dark current



(Credit: Hybrid SA, POLAR-2 collab.)



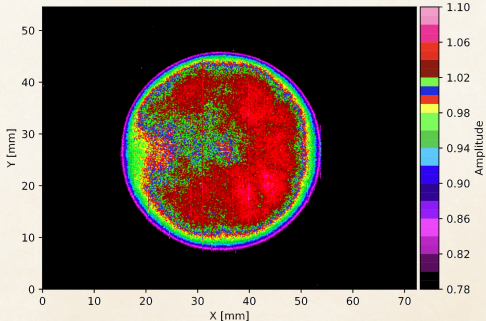
Exp. Astron. 55, p343–371 (2023)



# SiPM Thermal Annealing Probe Station Setup



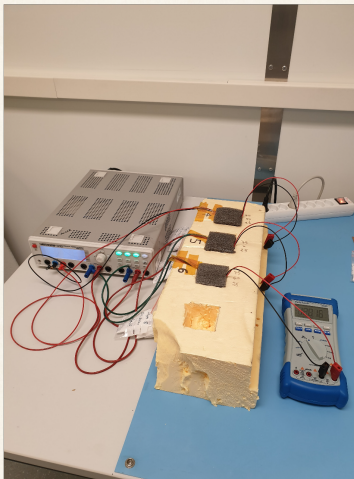
- ⊕ NIM A 1048 (2023) 167934
- ⊕ 58 MeV proton beam @IFJ-PAN, Krakow
- ⊕ Sensors exposed to 0.134 Gy (equivalent to 1.7 yrs on the CSS according to Geant4 simulations)
- ⊕ Fluence of  $10^8$  p/cm<sup>2</sup>





# SiPM Thermal Annealing Sensors Storage Setups

- 21 S13360-60xx SiPMs from Hamamatsu (25, 50, and 75  $\mu\text{m}$ ) stored at 6 temperatures ranging from  $-22.8 \pm 1.8^\circ\text{C}$  to  $48.7 \pm 3.3^\circ\text{C}$
- 4 of the sensors are stored with a bias ( $\Delta V = 3, 8, 12$  V)





# SiPM Thermal Annealing Probe Station Setup

Vacuum control  
for positioners  
and chuck

Positioners  
and probes

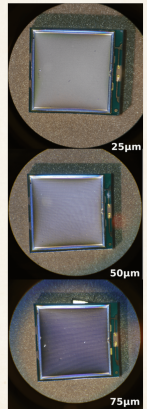
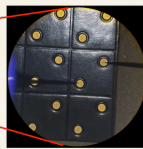
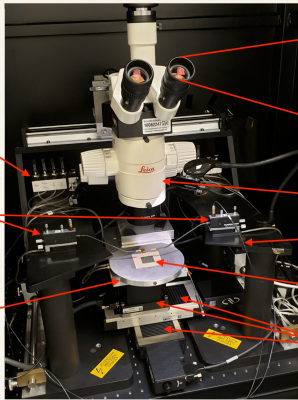
Chuck

Microscope

to HV power supply

SiPM chip

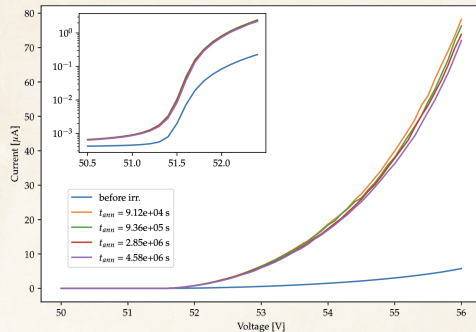
x, y and z motors





# I-V measurement versus time

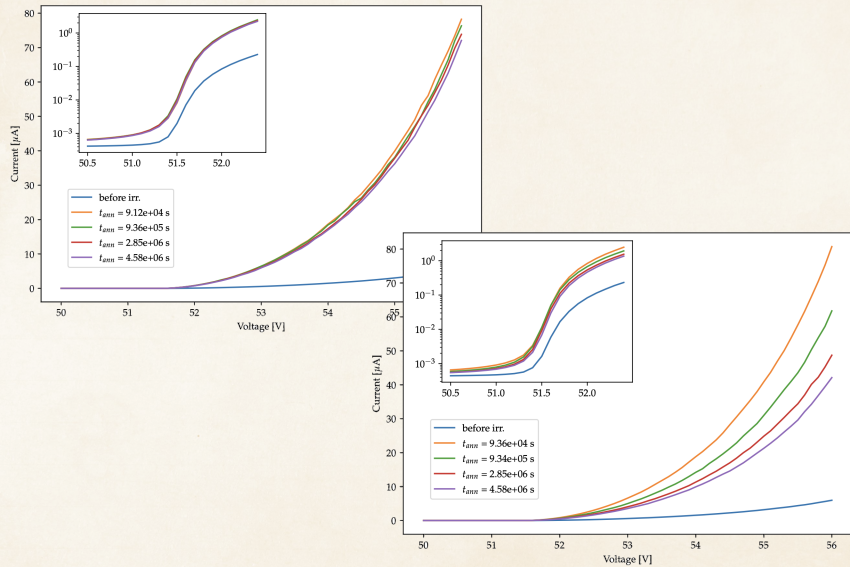
S13360-6075PE,  $-22.8 \pm 1.8^\circ\text{C}$  vs.  $20.5 \pm 0.6^\circ\text{C}$





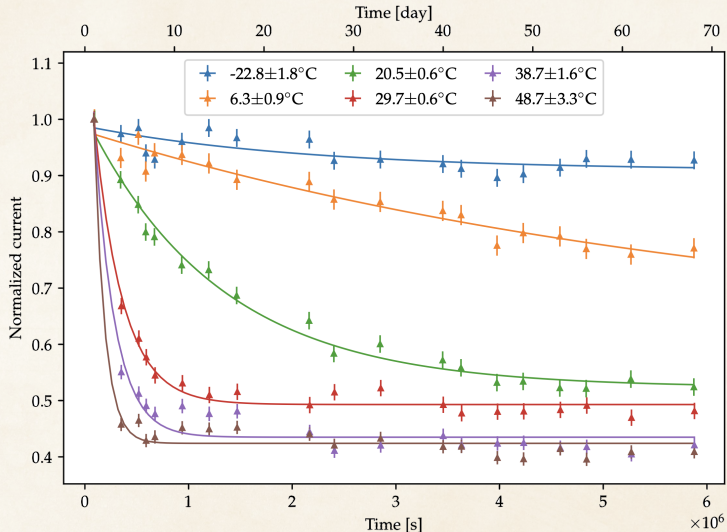
# I-V measurement versus time

S13360-6075PE,  $-22.8 \pm 1.8^\circ\text{C}$  vs.  $20.5 \pm 0.6^\circ\text{C}$



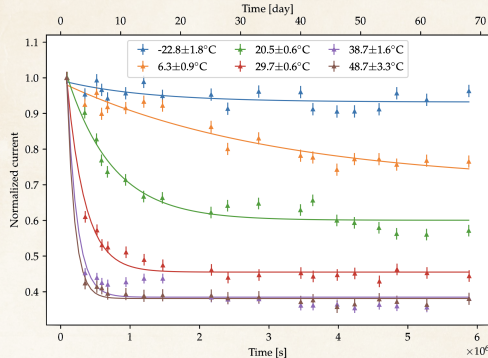


# Time evolution of dark current at $\Delta V=3$ V 75 $\mu\text{m}$ microcells



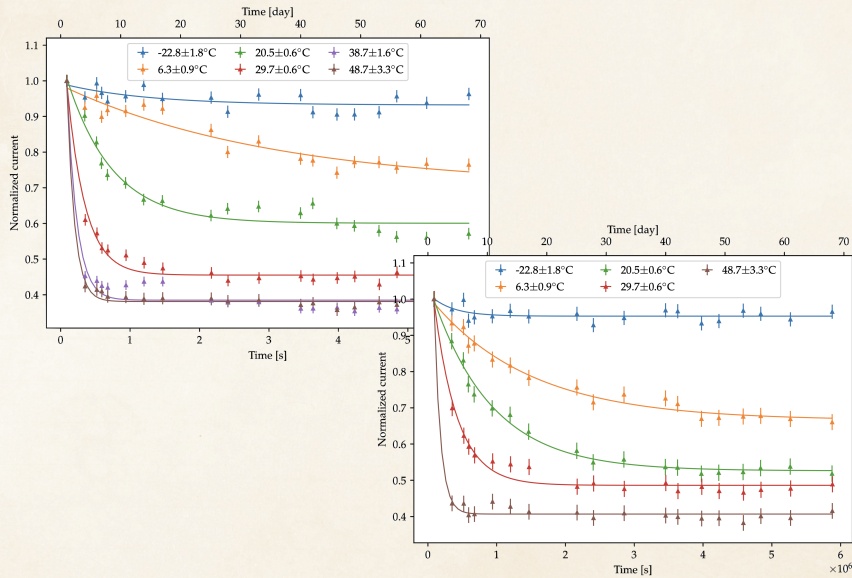


# Time evolution of dark current at $\Delta V=3$ V 25 and 50 $\mu\text{m}$ microcells



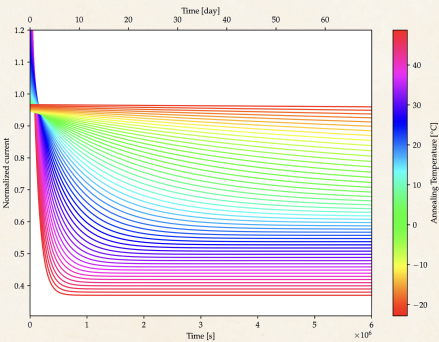
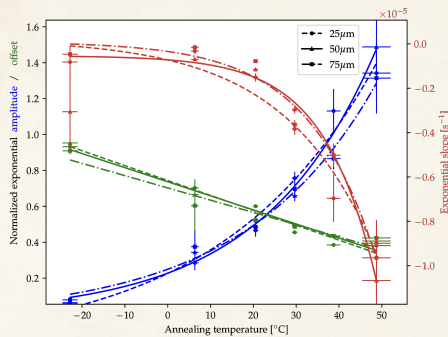


# Time evolution of dark current at $\Delta V=3$ V 25 and 50 $\mu\text{m}$ microcells



# Exponential decay parameters vs. T<sub>annealing</sub>

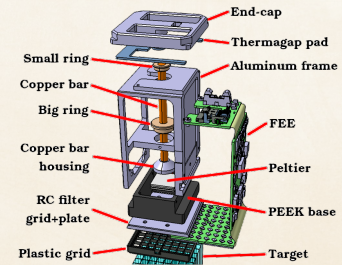
$$a(T) \times \exp(b(T) \cdot t) + c(T)$$



# Annealing strategies for POLAR-2

- 💡 SiPMs are being operated as cold as possible during scientific data taking thanks to a Peltier based active cooling system
- 💡 About once a year, the sensors can be annealed for a couple of days using power resistors (1.98 W @ 9 V) mounted on the back of the PCB
- 💡 Without annealing, the DCR is expected to increase by a factor 5 per year. This corresponds to an energy threshold increase of 0.75 keV for a SiPM intrinsic crosstalk of 10%. This number is halved with 1 day of annealing at 50°C every year.

Operating temperature [°C]	-10	0	20
Scenario 1 "No Annealing"	25µm	15.7 ± 0.8	
	50µm	15.4 ± 2.2	
	75µm	7.2 ± 0.9	
Scenario 2 "Continuous annealing"	25µm	13.15 ± 0.73	11.93 ± 0.67
	50µm	12.74 ± 1.84	11.61 ± 1.67
	75µm	5.80 ± 0.72	5.36 ± 0.65
Scenario 3a (1 day) "Continuous + Stimulated annealing"	25µm	8.02 ± 0.45	7.27 ± 0.41
	50µm	7.40 ± 1.07	6.75 ± 0.97
	75µm	3.59 ± 0.45	3.31 ± 0.40
			2.79 ± 0.34



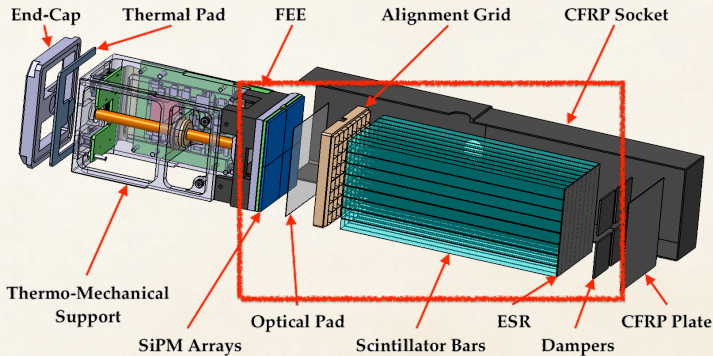


## Section 5

# Optical Characterization, Simulation, and Calibration of the POLAR-2 Polarimeter Modules

# Motivation Behind Optical Characterization

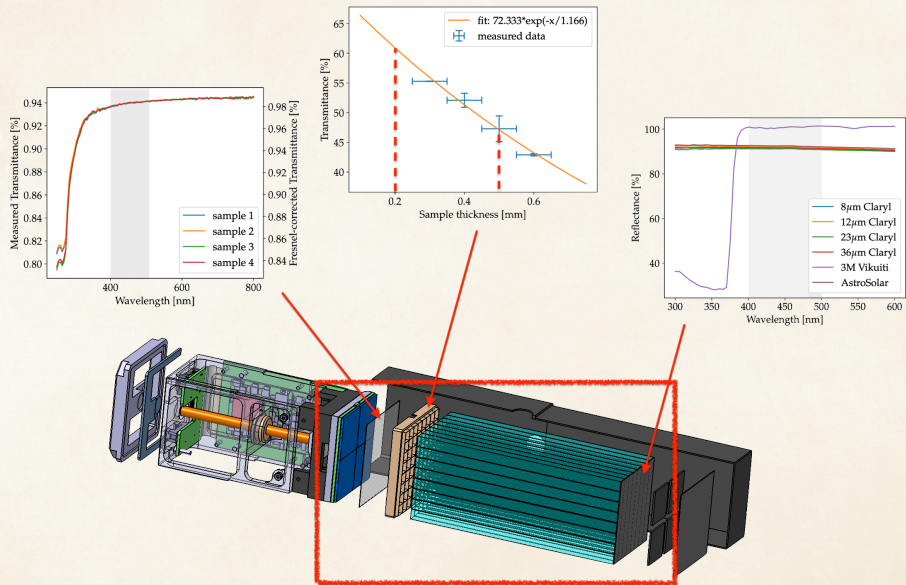
- ❖  $\gamma$ -rays gets converted into optical light in the scintillators, which gets collected by the SiPMs and converted into a measurable electrical signal pre-processed by the FEE
- ❖ The polarimeter module is therefore an optical system, and characterizing/simulation its optical behavior is crucial to understand/optimize the instrument performances





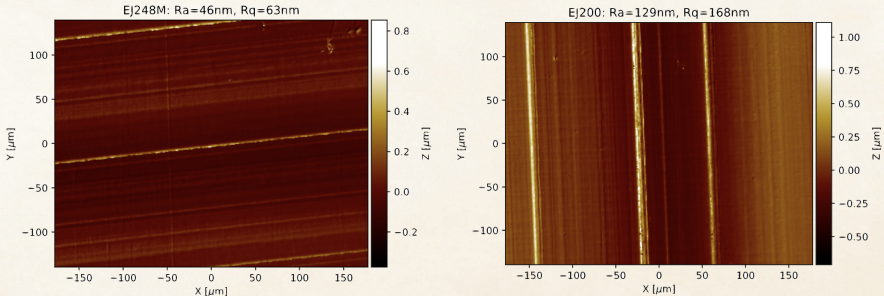
# Optical Characterization

## Reflectance and Transmittance measurements



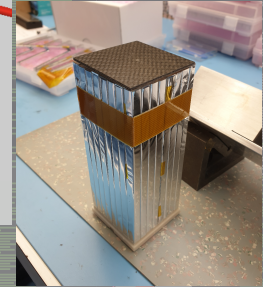
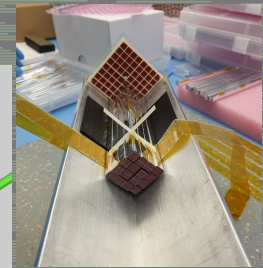
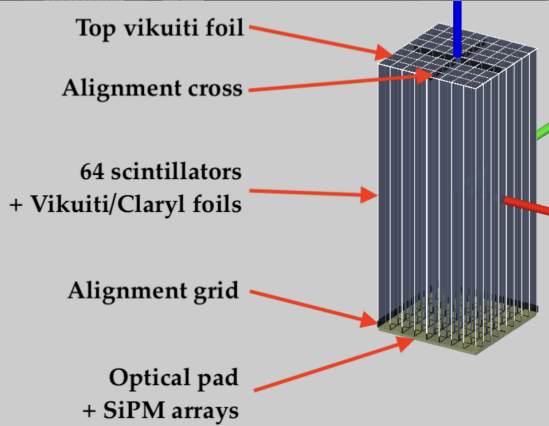
# Plastic Scintillator Surface Roughness

- 2 types of plastic scintillators investigated for the polarimeter: EJ-200 (10'000 photons/1 MeV  $e^-$ ) and EJ-248M (9'200 photons/1 MeV  $e^-$ ) from Eljen
- Module light yield is higher with EJ-248M!! Our guess: EJ-200 is slightly softer, more light loss at the interface due to rougher surface
- Surface quality measured for both scintillators at HEPIA using an Interferometric Optical Microscope





# Geant4 Optical simulations

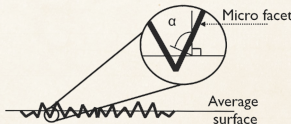
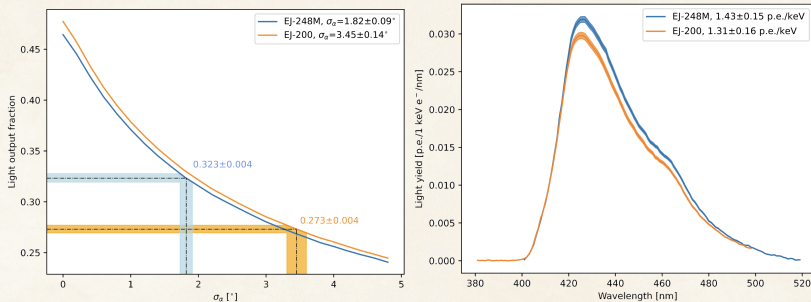




# Polarimeter Module Light Yield

## Optical Simulations vs. Measurements

- Great improvement compared to the 0.3 p.e./keV light yield in POLAR
- Allows to lower the energy threshold down to a few keV, significantly improves the statistics for a typical GRB spectrum

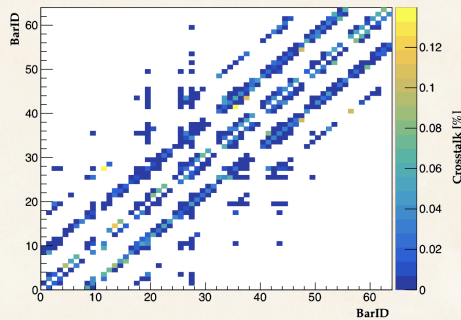
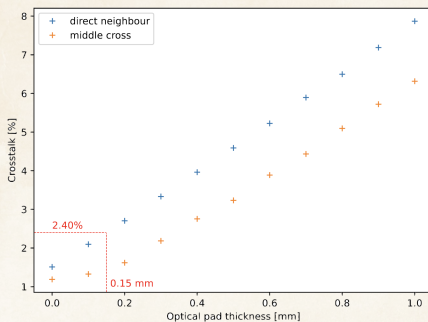


	$LY_{EJ-200}$ [p.e./keV]	$LY_{EJ-248M}$ [p.e./keV]
Measurement	$1.23 \pm 0.20$	$1.37 \pm 0.32$
Simulation	$1.31 \pm 0.16$	$1.43 \pm 0.15$



# Optical Crosstalk

## Optical Simulations vs. Measurements

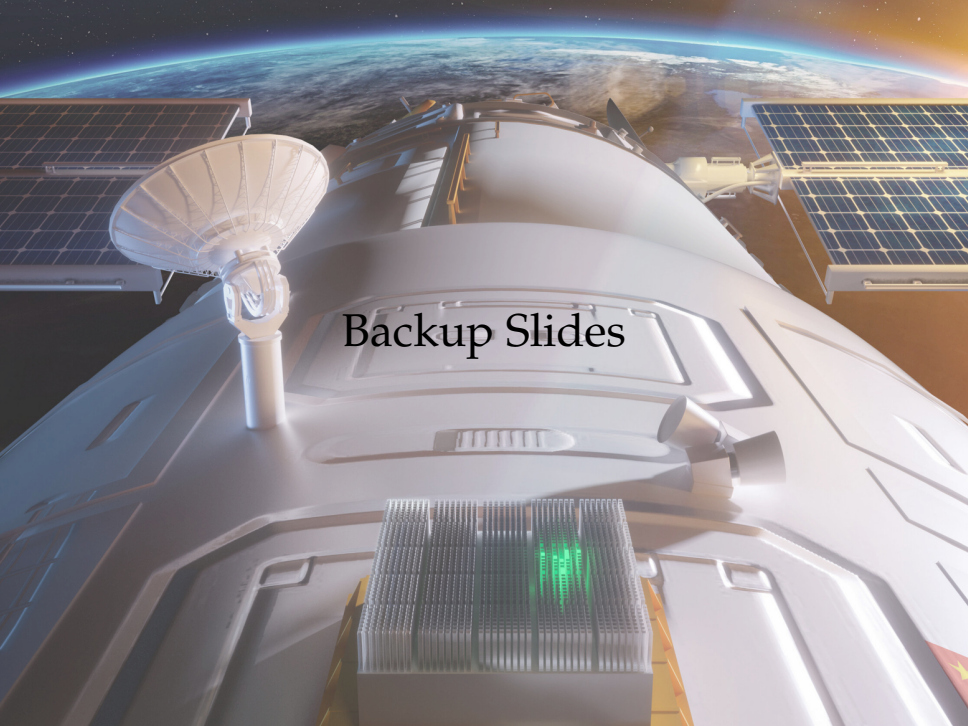


- Measurement compatible with simulations:  $P_{XT}=2.63 \pm 2.10\%$
- Compatible with expectation from simple calculation:  
 $3 \text{ mm}/125 \text{ mm} \times 60.9\% = 1.46\% \times 47.1\% = 1.13\%$  for middle cross)
- Optical crosstalk was  $\sim 15\%$  in POLAR: huge improvement thanks to the new wrapping technique and thinner SiPM entrance resin/opt. pad
- The improvement in optical crosstalk leads to a better sensitivity to polarization



# Overall Summary

- ❖ GRBs are the most powerful events in the universe since the Big-Bang, and as such are a unique place to study physics in extreme environments.
- ❖ Measuring the polarization of GRB prompt emission is thought as a very powerful way of answering the main questions about GRB physics.
- ❖ POLAR was launched in 2016 in order to answer these questions. It reported the measurement of low polarization levels for 14 GRBs, with a hint for time evolving polarization angle in the GRB pulse.
- ❖ An energy-resolved analysis of the polarization was conducted, and no significant energy dependence of the PD or PA was observed.
- ❖ The main limiting factor in POLAR is statistics. A four times bigger successor instrument, POLAR-2, is under development.
- ❖ One of the main upgrades from POLAR to POLAR-2 is the use of SiPMs instead of PMTs, which have better sensitivity. These silicon based sensors are subject to radiation damage. In order to recover part of their original scientific performances, thermal annealing can be employed. Thermal annealing was characterized using irradiated SiPMs stored at various temperatures.
- ❖ The POLAR-2 polarimeter module design was optimized thanks to characterization of individual optical elements and reliable Geant4 optical simulations. A light yield of  $\sim 1.5$  p.e./keV was reached (5 times higher than POLAR), while the optical crosstalk was reduced from  $\sim 15\%$  down to  $\sim 2.5\%$ .

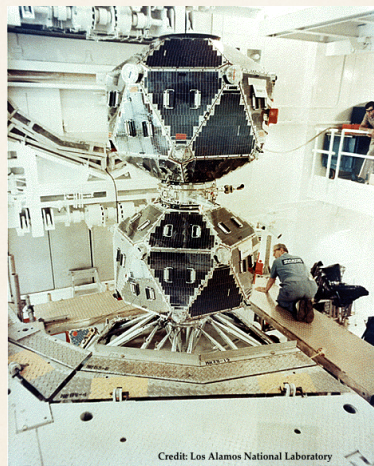
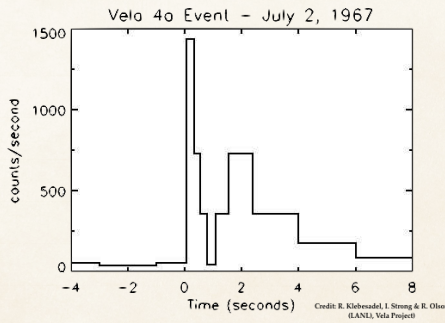


Backup Slides



# Discovery of GRBs

- Project Vela from USAF monitoring compliance to the Partial Test Ban Treaty of 1963
- First GRB detected on July 2<sup>nd</sup>, 1967 by Vela-4A, made public 7 years later
- Publication of 16 GRBs in 1973 by Klebesadel et al.



Credit: Los Alamos National Laboratory



# GRB Spectrum

## Band and CPL functions

GRBs are usually spectrally described by a Band function (Band+93):

$$N_E(E) = \begin{cases} A\left(\frac{E}{100 \text{ keV}}\right)^\alpha e^{-E/E_0} & \text{if } (\alpha - \beta)E_0 \geq E; \\ A\left(\frac{(\alpha-\beta)E_0}{100 \text{ keV}}\right)^{\alpha-\beta} e^{\beta-\alpha} \left(\frac{E}{100 \text{ keV}}\right)^\beta & \text{if } (\alpha - \beta)E_0 \leq E. \end{cases}$$

Their spectrum can sometimes be better fitted with a Cut-off Power-Law (CPL) function:

$$N_E(E) = K \left( \frac{E}{100 \text{ keV}} \right)^{-\alpha} e^{-E/E_c}$$

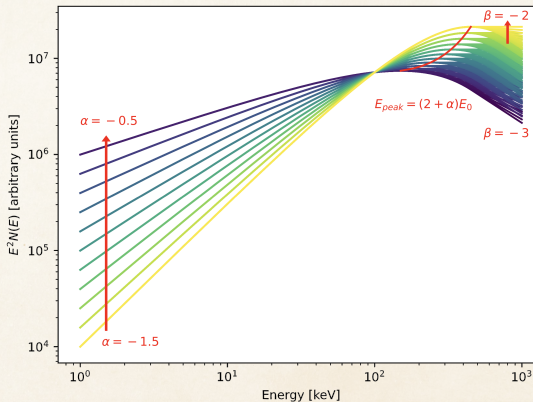


# GRB Spectrum

## The Band Function

GRBs are typically described by a non-thermal spectrum parameterized by the empirical Band function (smoothly joined broken power-laws):

$$N_E(E) = \begin{cases} A \left( \frac{E}{100 \text{ keV}} \right)^\alpha e^{-E/E_0} & \text{if } (\alpha - \beta)E_0 \geq E; \\ A \left( \frac{(\alpha - \beta)E_0}{100 \text{ keV}} \right)^{\alpha - \beta} e^{\beta - \alpha} \left( \frac{E}{100 \text{ keV}} \right)^\beta & \text{if } (\alpha - \beta)E_0 \leq E. \end{cases}$$





# GRB Jet Structure

⊗ Top-Hat (uniform) Jet (THJ):

$$\frac{L'_{\nu'}(\theta)}{L'_{\nu',0}} = \frac{\Gamma(\theta)}{\Gamma_0} = \begin{cases} 1 & \text{if } \theta \leq \theta_j; \\ 0 & \text{if } \theta > \theta_j. \end{cases}$$

⊗ Smoothed Jet: Exponential and Power Law Wings ( $\xi_j \equiv (\Gamma\theta_j)^2$ )

$$\frac{L'_{\nu'}}{L'_{\nu',0}} = \begin{cases} 1 & \text{if } \xi \leq \xi_j; \\ \exp [(\sqrt{\xi_j} - \sqrt{\xi})/\Delta] & \text{if } \xi > \xi_j. \end{cases} \quad \frac{L'_{\nu'}}{L'_{\nu',0}} = \begin{cases} 1 & \text{if } \xi \leq \xi_j; \\ \left(\frac{\xi}{\xi_j}\right)^{-\delta/2} & \text{if } \xi > \xi_j. \end{cases}$$

⊗ Truly structured Jet: Gaussian Jet (GJ)

$$\frac{L'_{\nu'}(\theta)}{L'_{\nu',0}} = \frac{\Gamma(\theta) - 1}{\Gamma_c - 1} \propto \exp\left(-\frac{\theta^2}{2\theta_c^2}\right)$$

⊗ Truly structured Jet: Power Law Jet (PLJ)

$$\frac{L'_{\nu'}(\theta)}{L'_{\nu',0}} = \Theta^{-a}, \quad \frac{\Gamma(\theta) - 1}{\Gamma_c - 1} = \Theta^{-b}, \quad \Theta \equiv \sqrt{1 + \left(\frac{\theta}{\theta_c}\right)^2}$$



# GRB Outflow Composition & Dynamics

$$\sigma \equiv \frac{w'_B}{w'_m} = \frac{B'^2}{4\pi \left( \rho' c^2 + \frac{\hat{\gamma}}{\hat{\gamma}-1} P' \right)}$$

- ⊗  $w'_B = B'^2 / 4\pi$  is the magnetic field enthalpy
- ⊗  $w'_m = \rho' c^2 + \frac{\hat{\gamma}}{\hat{\gamma}-1} P'$  is the matter enthalpy
- ⊗ Kinetic Energy Dominated (KED) flow:  $\sigma < 1$
- ⊗ Poynting Flux Dominated (PFD) flow:  $\sigma > 1$



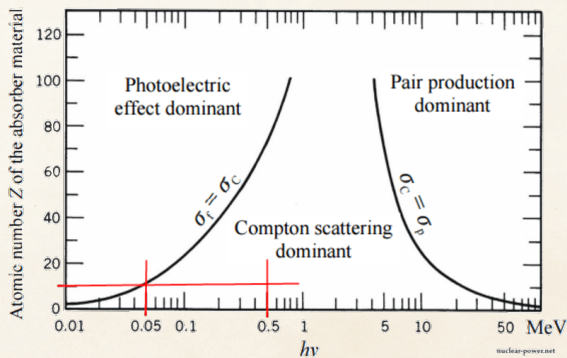
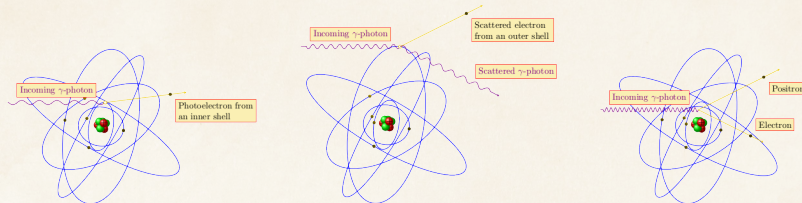
# Early GRB Polarization Measurements

GRB	Instrument	Energy (keV)	PD (%)
021206	RHESSI	150-2000	$80 \pm 20\%$
021206	RHESSI	150-2000	<100%
021206	RHESSI	150-2000	$41^{+57\%}_{-44\%}$
930131	CGRO/BATSE	20-1000	35-100%
960924	CGRO/BATSE	20-1000	50-100%
041219A	INTEGRAL/SPI	100-350	$98 \pm 33\%$
041219A	INTEGRAL/SPI	100-350	$96 \pm 40\%$
041219A	INTEGRAL/IBIS	200-800	$43 \pm 25\%$
061122	INTEGRAL/SPI	100-1000	< 60%
100826A	IKAROS/GAP	70-300	$27 \pm 11\%$
110301A	IKAROS/GAP	70-300	$70 \pm 22\%$
110721A	IKAROS/GAP	70-300	$80 \pm 22\%$
061122	INTEGRAL/IBIS	250-800	> 60%
140206A	INTEGRAL/IBIS	200-800	> 48%
151006A	Astrosat/CZTI	100-300	-
160530A	COSI	200-5000	< 46%

from McConnell 2016

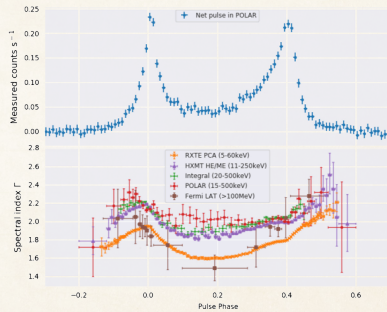


# Low-Z scintillators Optimized for Compton Scattering



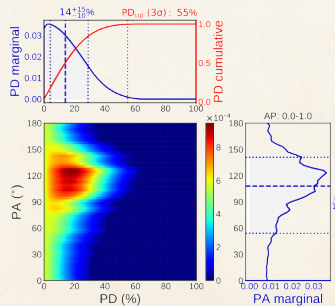
# Crab pulsar results from POLAR

- ❖ Exposition of 400 h for spectral analysis, 1222 h for polarization analysis
- ❖ Nebula contribution subtracted, 3 pulse intervals studied: AP (0.0–1.0), P1 (0.0–0.2 || 0.8–1.0) and P2 (0.2–0.6)



Journal of High Energy Astrophysics 24 (2019) 15–22

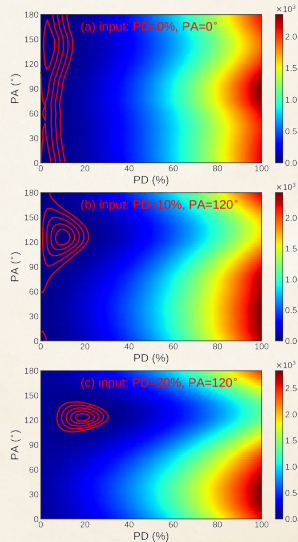
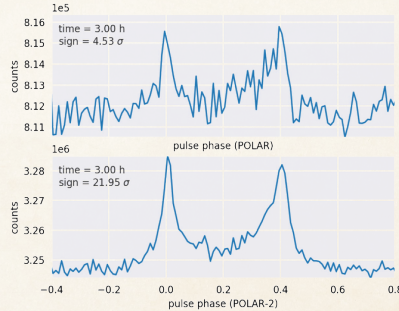
	PD [%]	PA [°]
AP	$14^{+15}_{-10}$	$108^{+33}_{-54}$
P1	$17^{+18}_{-12}$	$174^{+39}_{-36}$
P2	$16^{+16}_{-11}$	$78^{+39}_{-30}$



MNRAS 512, 2827–2840 (2022)

# Crab predictions for POLAR-2

- ❖ POLAR spectral fitting:  $\sim 400\text{h}$ ,  $58.14\sigma \rightarrow$  will be achieved with 33h POLAR-2 exposure
- ❖ 2yrs of POLAR-2 data  $\implies$  more detailed spectral analysis of the Crab pulsar, and even of other PSRs (e.g. PSR B1509-58)
- ❖ If Crab pulsar is unpolarized:  $5\sigma$  upper limits on the PD to a level of  $\sim 20\%$ . If Crab pulsar is 10 or 20% polarized, it will be confirmed with  $5$  or  $4\sigma$

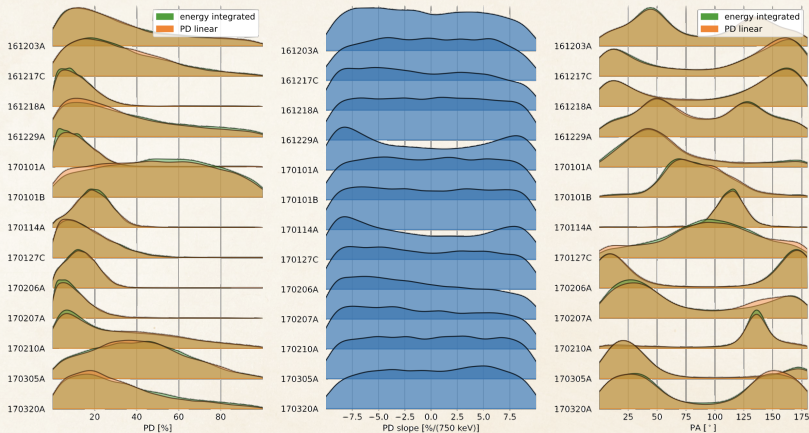




# Energy resolved results: POLAR catalog

## Linear fit of the PD

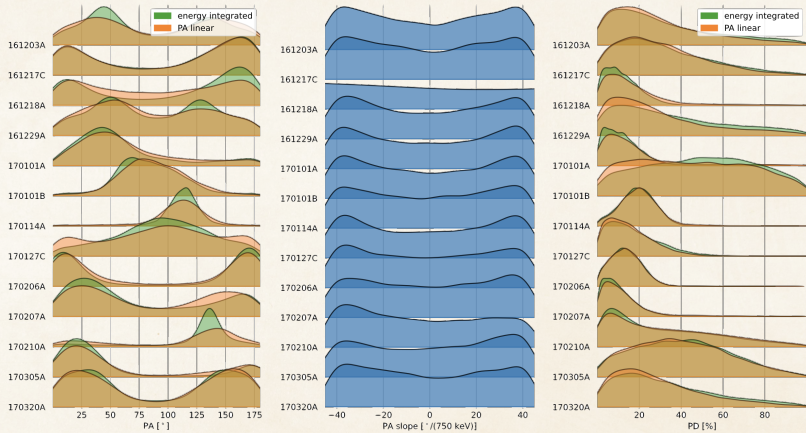
$$PD = PD_{intercept} + PD_{slope} \times \frac{E}{E_{max}} ; \quad E_{max} = 750 \text{ keV} ; \quad PA = cst.$$



# Energy resolved results: POLAR catalog

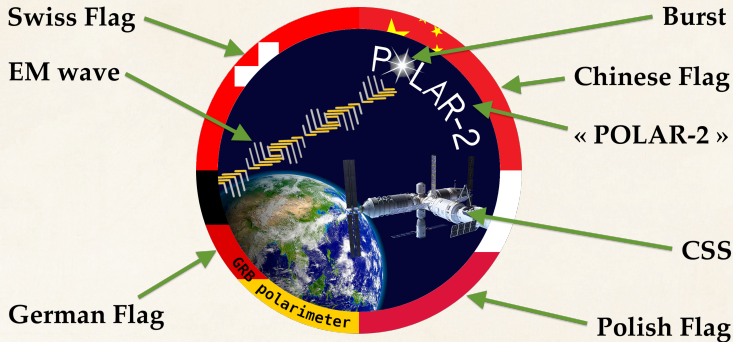
## Linear fit of the PA

$$PA = PA_{intercept} + PA_{slope} \times \frac{E}{E_{max}} ; \quad E_{max} = 750 \text{ keV} ; \quad PD = cst.$$

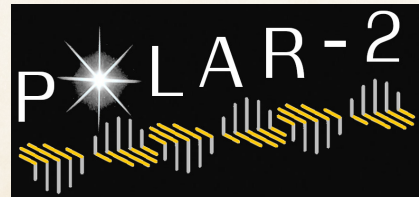




# POLAR-2 Logos



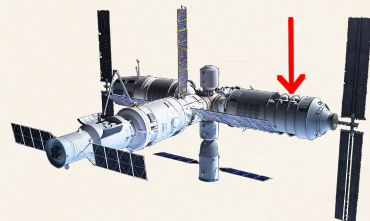
Simplified logo for PCBs:



# Enhanced POLAR-2: LPD and BSD

Two other payloads proposed to the China Space Station (CSS):

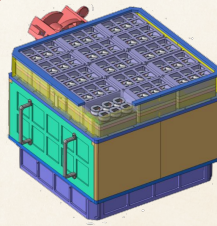
X-ray Polarimeter (LPD) lead by  
GuangXi University, Nanning  
& Broad-band Spectrometer (BSD)  
lead by IHEP, Beijing



➤ Low-energy Polarization Detector:

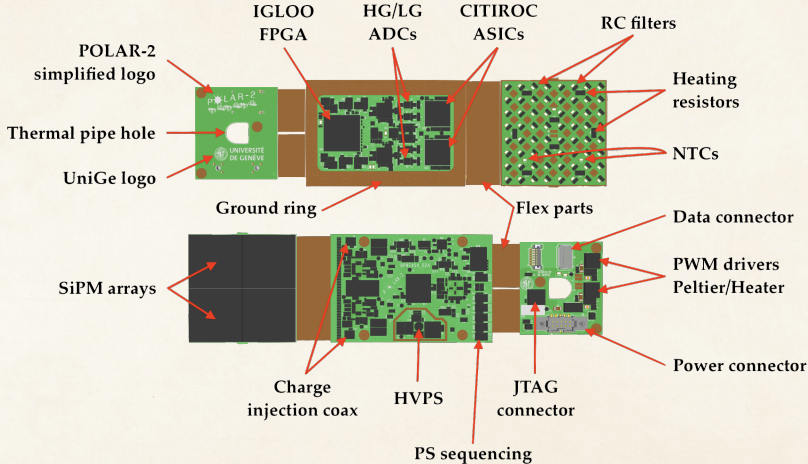
LPD

- ~2-10 keV X-ray polarimetry
- Broad energy-band Spectrum Detector: BSD
- ~10-2000keV
- Accurate GRB localization and spectroscopy for HPD and LPD
- Status: Selected, to be adopted



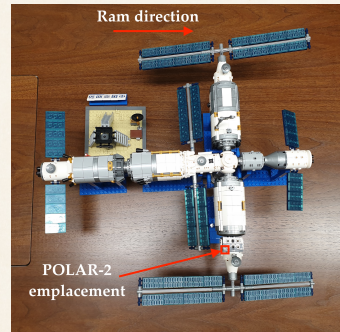
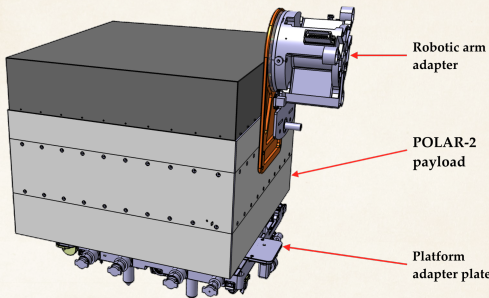
from Jianchao Sun, IHEP

# POLAR-2 Front-End Electronics



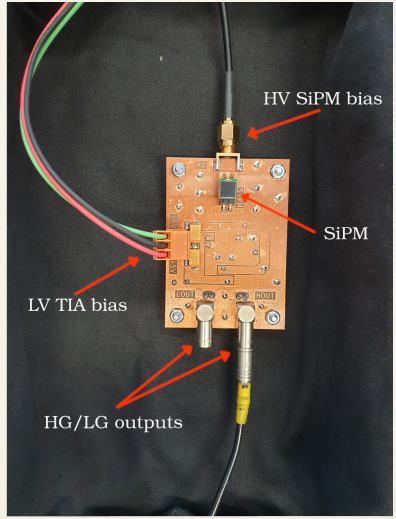


# POLAR-2 Mounting on the CSS



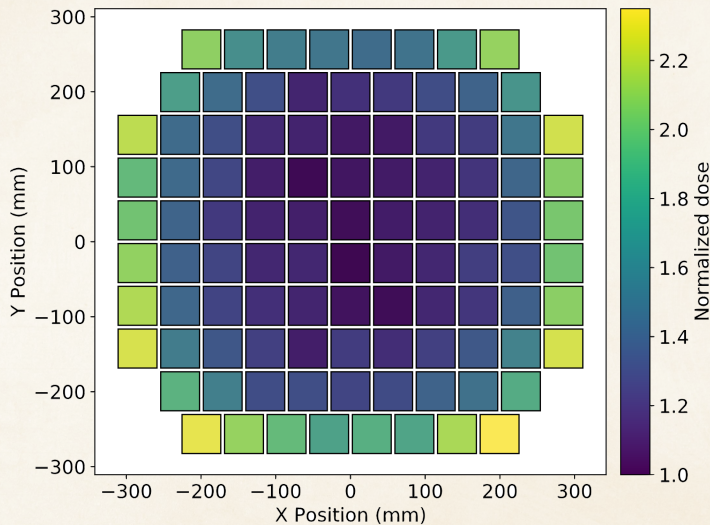


# SiPM Thermal Annealing DCR Measurement Setup



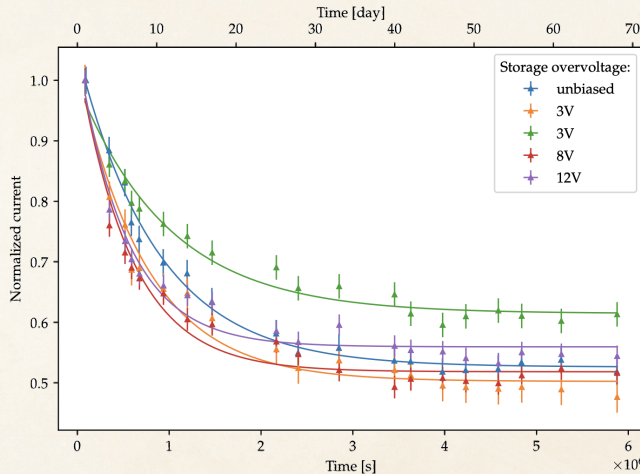


# SiPM Dose Map POLAR-2



# Annealing with biased sensors

Behavior is the same as for unbiased SiPMs (S13360-6050PE):

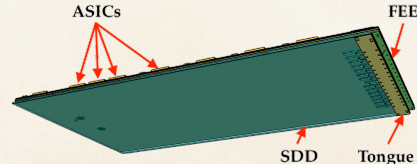
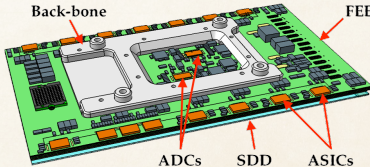
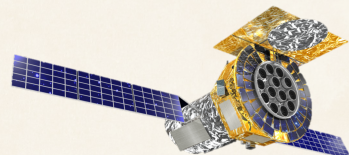




# eXTP Instrument Design

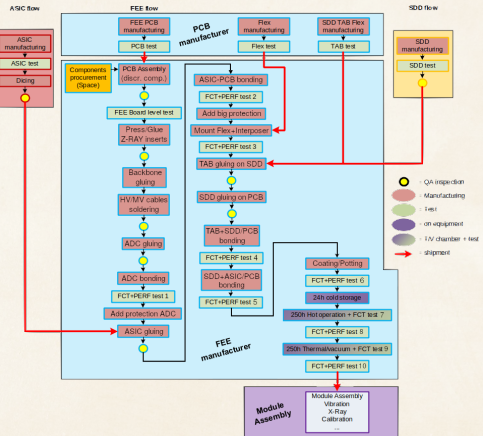
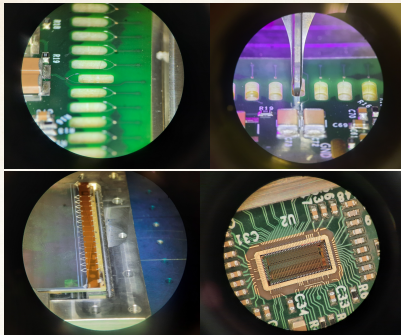
The enhanced X-Ray Timing and Polarimetry mission (eXTP) will be composed of:

- ❖ **Large Area Detector (LAD):** effective area of  $3.4 \text{ m}^2$  in the 6-10 keV range, FoV  $< 1^\circ$ , full range 2-30 keV, energy res. of 250 eV at 6 keV
- ❖ **Spectroscopic Focusing Array (SFA):** 0.5-10 keV, 9 X-ray optics of  $12'$  FoV each, time resolution of  $10 \mu\text{s}$
- ❖ **Polarimetry Focusing Array (PFA):** based on imaging GPD, polarimetry in 2-10 keV
- ❖ **Wide Field Monitor (WFM):** 6 coded mask cameras, FoV of  $3.7 \text{ sr}$  in 2-50 keV



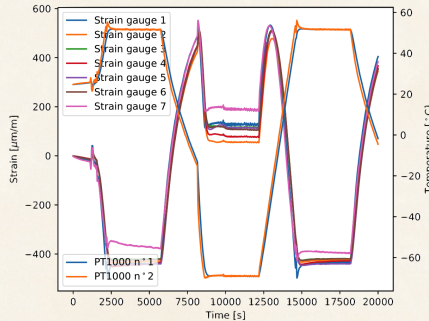
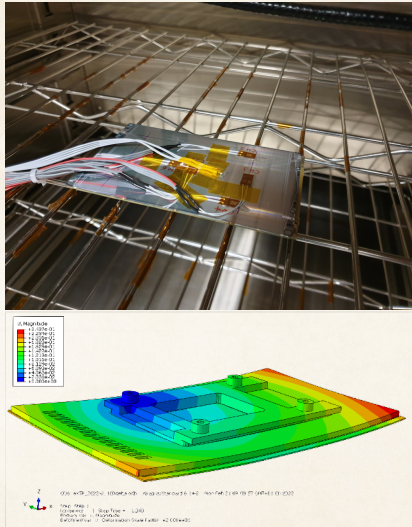


# eXTP LAD Detector Assembly



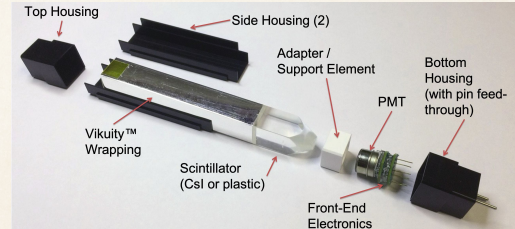
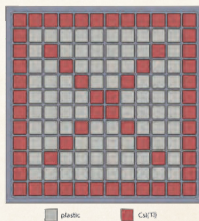
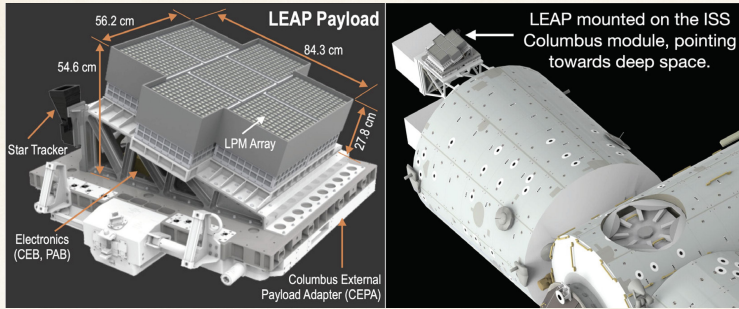


# eXTP LAD Thermal Cycling



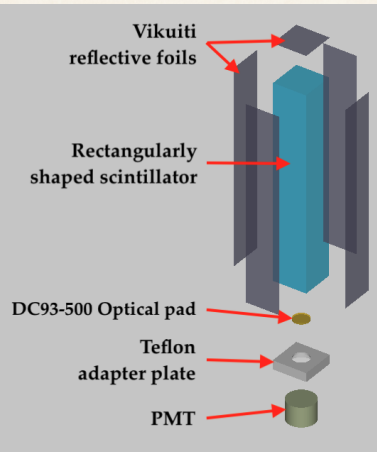
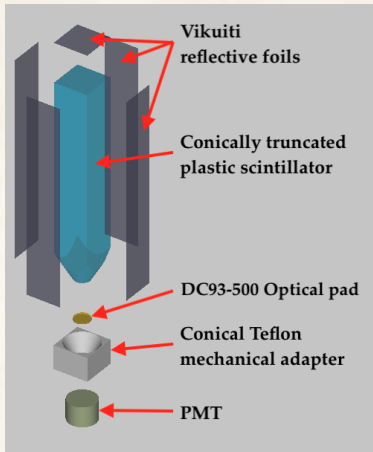


# LEAP design





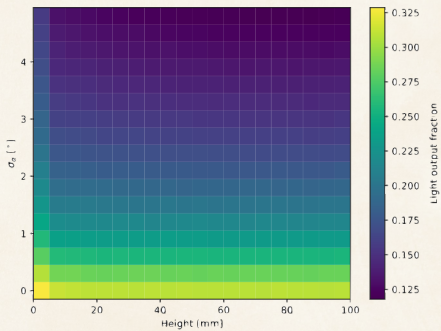
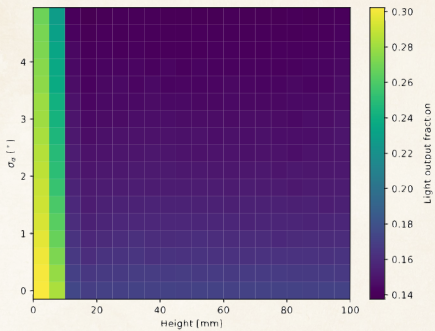
# LEAP PDE Optical Simulation





# Simulated LEAP Light Output

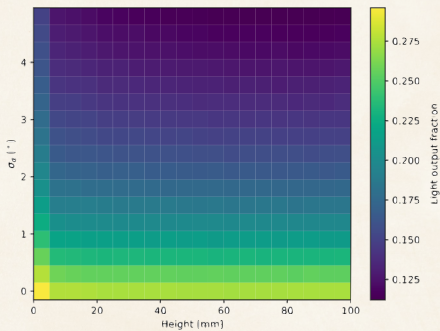
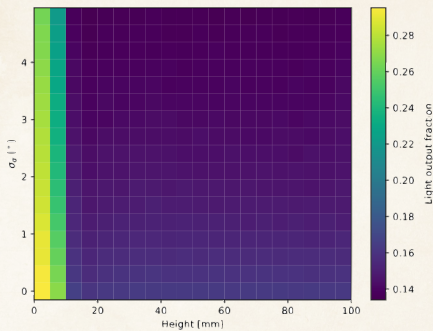
## EJ-200





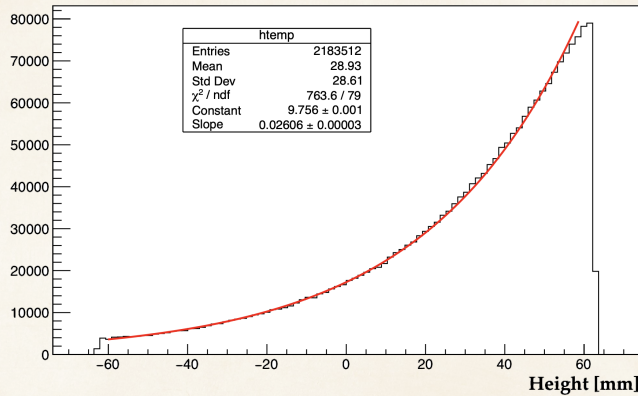
# Simulated LEAP Light Output

## EJ-248M





# Simulated LEAP Light Output Comparison



---

	EJ-200	EJ-248M
Conically tapered bar	$14.21 \pm 0.04\%$	$14.40 \pm 0.04\%$
Square bar	$13.85 \pm 0.04\%$	$17.71 \pm 0.04\%$

---